Interaction between shock waves and supersonic boundary layers over forward-facing and backward-facing steps

Weibo Hu, Bas van Oudheusden, Stefan Hickel[1]

[1]Aerodynamics Group, Faculty of Aerospace Engineering, Delft University of Technology

Introduction

Shock wave / boundary layer interactions (SWBLI) have been an active research topic in the aerospace community over the past decades. SWBLI form a dynamic system of mutually interacting boundary layers, free shear layers, shock waves, an expansion fan, and a separation bubble. It is widely reported that this dynamic system features a significant low-frequency unsteadiness, whose frequency is typically two orders lower than the characteristic frequency of the incoming turbulent boundary layer, and that may detrimentally affect the structural integrity of aircraft and rockets. Several theories have been proposed to explain the origin of this unsteadiness. These theories can be classified based on whether they consider upstream and downstream mechanisms as the main driver (see [1] for an overview).

The validity and general applicability of these mechanisms is a scientific controversary. In literature, there is no consensus even for extensively studied canonical incident shock and compression ramp cases. In addition, these so-called upstream and downstream mechanisms may not apply in the same manner to more complex geometries, such as SWBLI over forward-facing steps (FFS) or backward-facing steps (BFS), in view of their different flow topology. To enhance our understanding of the underlying physical mechanisms, we performed extensive numerical studies on the low-frequency unsteady dynamics of SWBLI in laminar and turbulent supersonic FFS/BFS cases [2, 3, 4, 5]; the work as described here was part of the PhD thesis by the first author [6].

Flow configuration and computational method

We consider an open FFS and BFS (i.e., no upper wall) with the same supersonic freestream conditions at $Ma = 1.7$ and $Re = 1.37 \times 10^7$ m^{-1}. The incoming boundary layer is either a fully laminar flow, a laminar flow superimposed with linear instability modes with different amplitude, or a fully turbulent boundary layer. Common to all cases of this study is Re_δ = 13718, based on the 99% velocity boundary layer thickness δ_0 at the inlet.

We employ the large eddy simulation (LES) method of Hickel et al. [7] and the finite volume solver INCA (www.inca-cfd.com). INCA is a mature solver that has been extensively applied and validated for various compressible flow cases, including SWBLI at compression ramps and SWBLI on planar walls. INCA uses adaptive block-Cartesian meshes with hanging nodes at block interfaces to accommodate adaptive mesh refinement (AMR). For the current simulations, the mesh resolution is uniform within each block except in blocks near walls, where hyperbolic grid stretching is used, such that the mesh resolution is $y^+ < 1$ in the wall-normal direction. For fully turbulent cases, inflow conditions are provided by the digital filter technique of Klein et al. [8]. The step and wall are modelled as no-slip adiabatic surfaces. Non-reflecting freestream boundary conditions based on Riemann invariants are used and periodic boundary conditions are imposed in the spanwise direction. For more details on the setup, see [2, 3, 4, 5, 6].

Selected results

Mean and instantaneous flow

The mean flow field in Figure 1 provides an overview of the main flow topology, including a centred Prandtl-Meyer expansion from the step edge, the separation bubble and shock waves. For the FFS case, the boundary layer separates at x/δ_0 = 15.9 and reattaches on the step wall at y/δ_0 = 2.1. The separation region is encompassed by two shocks, i.e., the separation and reattachment shock. In contrast, the flow over the BFS separates at the step edge and reattaches at x/δ_0 = 8.9, and there is only a reattachment shock that originates from the compression waves near the reattachment. Figure 2 shows instantaneous vortical structures for a transitional case with laminar inflow and for a fully turbulent case. From the instantaneous flow fields in Figure 3, two main types of unsteady behaviour are observed: a global motion involving the breathing of the separation bubble and the flapping of the shock and a relatively localized unsteadiness related to the shedding of vortices along the shear layer.

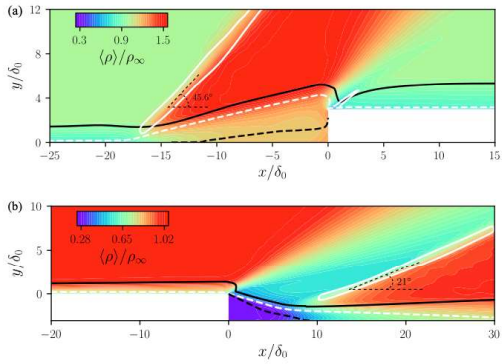

Figure 1: Density contours of the time- and spanwise- averaged flow field for two turbulent cases: (a) FFS and (b) BFS (the flow is from left to right). The black dashed line represents $u = 0$ and visualizes the separation bubble, the black solid line shows the boundary layer edge, and the white dashed line is the sonic line ($Ma = 1$). The separation shock (FFS) and reattachment shocks (FFS and BFS) are visualized by white solid lines, which enclose regions of large pressure gradients.

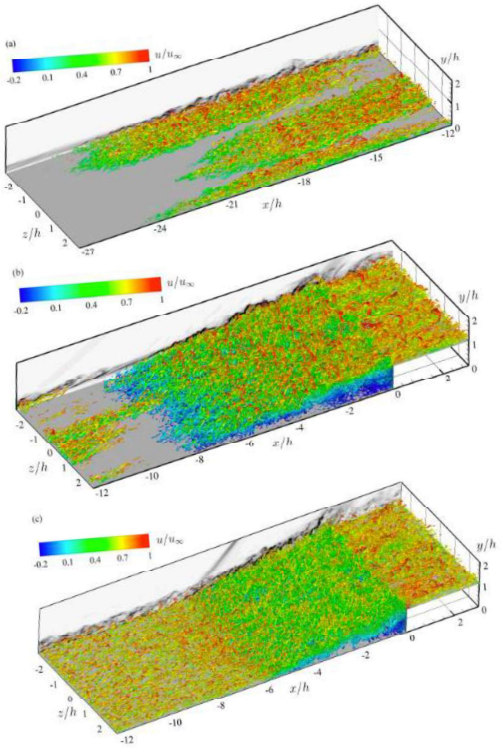

Figure 2: Instantaneous vortical structures for (a, b) a transitional case with laminar inflow and (c) a fully turbulent FFS case.

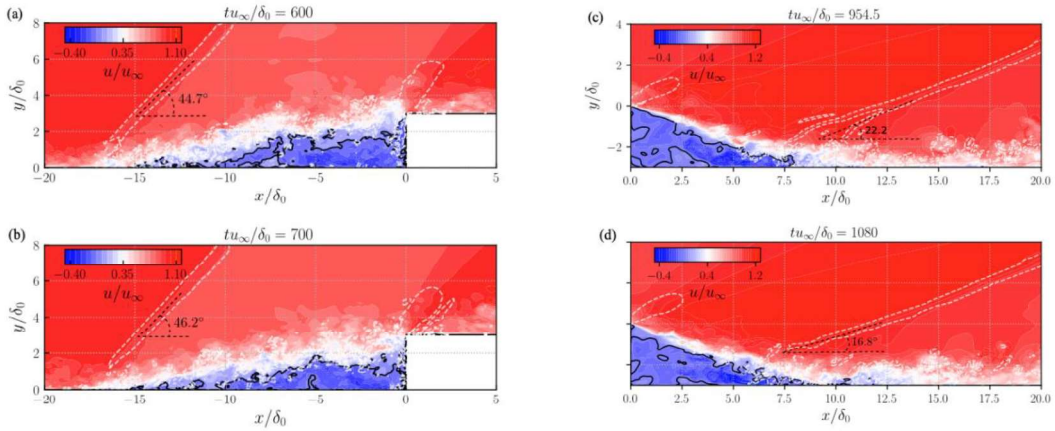

Figure 3: Contours of the instantaneous streamwise velocity for two turbulent cases. (a) FFS: $t\,u_\infty/\delta_0$ = 600, (b) FFS: $t\,u_\infty/\delta_0$ = 700, (c) BFS: $t\,u_\infty/\delta_0$ = 955, and (d) BFS: $t\,u_\infty/\delta_0$ = 1080. Black solid lines denote the isolines of $u = 0$ and white dashed lines signify the isolines of $|\nabla p|\delta_0/p_\infty$ = 0.4.

Spectral analysis

The frequency weighted power spectral density (FWPSD) of the wall pressure in Figure 4 shows a broadband frequency spectrum in these two unsteady SWBLI systems. Two distinct low-frequency ranges are identified from the spectral map, i.e., a lower one ($0.005 \le f\ \delta_0/u_\infty \le 0.05$ for the FFS and $0.06 \le f\ \delta_0/u_\infty \le 0.08$ for the BFS) and a medium one ($0.06 \le f\ \delta_0/u_\infty \le 0.25$ for the FFS and $0.1 \le f\ \delta_0/u_\infty \le 0.3$ for the BFS). The energetic low-frequency range is in good agreement with results for incident shock and ramp SWBLI cases (Priebe and Martin [9]; Pasquariello et al. [10]), which is widely reported to be approximately two orders lower than the characteristic frequency of the incoming energetic turbulent scales u_∞/δ_0.

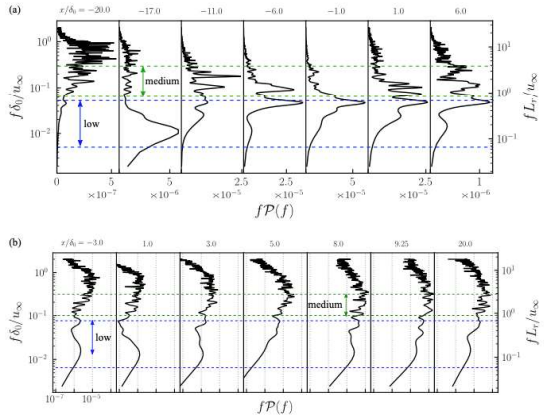

Figure 4: Frequency weighted power spectral density of the wall pressure with the streamwise distance for two fully turbulent (a) FFS and (b) BFS cases.

To further scrutinize the physical links between various dynamics and frequencies of the unsteady motions, several typical flow parameters, including the reattachment location, separation bubble volume and shock angle, were extracted from the present results. The FWPSD of the reattachment location for turbulent FFS and BFS cases has a medium frequency peak located around 0.1 u_∞/δ_0, which suggests that the reattached shear-layer flow is related to the medium-frequency unsteadiness in SWBLI. The intermediate frequencies are associated with the passage of shedding vortices formed in the separated shear layer. The low-frequency unsteadiness is associated with the breathing of the separation bubble and flapping motion of the shock wave. The PSD for the volume of the separation bubble shows a single spectral peak at 0.2 $u_\infty/\delta_0$for both FFS and BFS cases. Similarly, the motions of the shock angle feature a dominant low frequency.

Dynamic mode decomposition

To further analyze the flow features that contribute to the unsteady dynamics at different frequencies, a dynamic mode decomposition (DMD) of the three- dimensional FFS and BFS flow fields was carried out based on snapshots for a spatial subdomain. For both the FFS and BFS cases, three branches of modes with different frequencies are identified from the DMD frequency spectrum.

For the FFS case, we selected one representative mode from each branch, based on the growth rate and magnitudes of the modes, marked as mode ϕ_1, ϕ_2, and ϕ_3. For the low-frequency mode ϕ_1 ($f\delta_0/u_\infty$ = 0.013), iso-surfaces of the modal pressure fluctuations show significant structures around the separation shock and compression waves caused by the reattachment. The variation of the large structures with the phase angles indicates the unsteady motions of the shock both in the spanwise and streamwise direction. Considering the modal velocity fluctuations for the same mode in Figure 5, iso-surfaces of u'/u_∞= 0.2 visualize the counter-rotating streamwise Görtler vortices, distributed from the free shear layer to downstream of the reattachment point. In addition, we also determined the variation of the Görtler number G_t along the streamlines, and found that values larger than the critical value (G_t= 0.6) occur near the separation and reattachment region, suggesting a strong Görtler instability in the interaction region. These observations suggest that the low-frequency flapping motions of the shock are related to streamwise-elongated Görtler vortices in the present case. These unsteady longitudinal vortices are usually induced by the centrifugal forces from the strong curvature of the streamlines in the separation region, which provides a potential physical mechanism for the low-frequency unsteadiness in this FFS case.

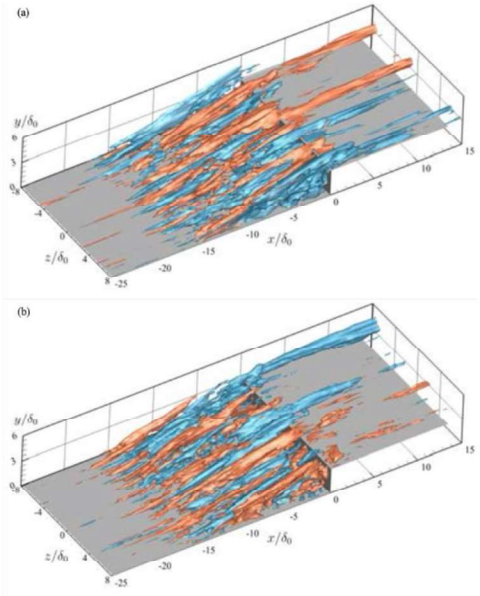

Figure 5: Iso-surfaces of the modal streamwise velocity fluctuations from DMD mode ϕ_1 with phase angle (a) $\theta = 0$ and (b) $\theta = 3\pi/4$ for a turbulent FFS case (orange: u'/u_∞= 0.2, blue: u'/u_∞= −0.2).

For the medium-frequency mode ϕ_2, the pressure iso-surfaces show high levels of modal fluctuations along the free shear layer. Positive and negative fluctuations are alternating in the streamwise direction, which represents the propagation of acoustic waves. The radiation of the acoustic waves is in agreement with the results from a global linear stability analysis of an impinging shock case in laminar regime. Regarding the modal fluctuations of the streamwise velocity, shown in Figure 6, Λ-shaped structures are observed in the free shear layer and alternate along both the spanwise and streamwise directions. Based on these observations, we believe this mode represents the convection of the shear layer vortices. Pasquariello et al. [10] addressed similar conclusions from the two-dimensional DMD analysis of a flat-plate, incident shock case at higher Reynolds number.

Similarly, for the BFS case, the flapping of the shock wave and counter-rotating Görtler vortices are responsible for the low-frequency motions, while the shedding vortices along the shear layer and the induced Mach-like waves contribute to the medium-frequency behaviour.

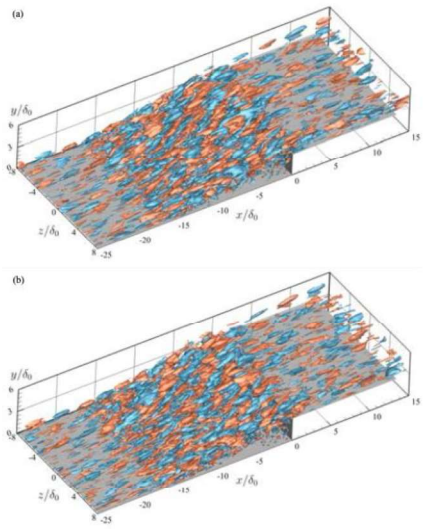

Figure 6: Iso-surfaces of the modal streamwise velocity fluctuations from DMD mode ϕ_2, with phase angle (a) $\theta = 0$ and (b) $\theta = 3\pi/4$ for a turbulent FFS case (orange: u'/u_∞= 0.2, blue: u'/u_∞= −0.2).

Conclusions

The low-frequency unsteady dynamics of SWBLI over forward-facing and backward-facing steps was investigated at $Ma = 1.7$ and Re_δ = 13718 using a well-resolved LES. The main flow topology of the SWBLI region contains shock waves (a separation shock in the FFS case and reattachment shocks in both cases), a main separation bubble and a centred Prandtl-Meyer expansion fan. The instantaneous visualizations indicate that the unsteady behaviour involves vortex shedding in the separated shear layer, breathing of the separation bubble, shock wrinkling, and flapping shock motions. From the spectral analysis, we observe broadband low-frequency motions in the interaction region, which can be classified into two branches based on their dominant frequency. Medium-frequency contents are associated with shear layer vortices, and the lower frequency dynamics is associated with the unsteady separation region.

Three-dimensional DMD analysis was applied to identify the individual single-frequency modes that have the largest contributions to the observed unsteady behaviour. Our results show a statistical link between the shock motions (shown by pressure fluctuations) and unsteady Görtler-like vortices (shown by the streamwise velocity fluctuations) along the shear layer. The medium-frequency modes represent the shedding of shear-layer vortices and the radiation of the induced Mach waves.

Based on the above observations and discussion, we believe that the physical mechanism of the low-frequency unsteadiness of SWBLI in FFS/BFS cases is similar as for other canonical SWBLI cases, i.e., unsteady Görtler-like vortices in the shear layer act as an unsteady forcing that is required to drive and sustain the low-frequency motions of shocks and separation bubble. A more detailed analysis is provided by Hu et al. [2, 3, 4, 5, 6].

Acknowledgments

This work was carried out on the Dutch national e-infrastructure with the support of SURF Cooperative and was partly financed by the Dutch Research Council (NWO) project number 2019.045.

References

1. Clemens, N. T., Narayanaswamy, V. (2014). Low-frequency unsteadiness of shock wave/turbulent boundary layer interactions. *Annual Review of Fluid Mechanics* **46**(1):469–492.
2. Hu, W., Hickel, S., van Oudheusden, B. (2019). Dynamics of a supersonic transitional flow over a backward-facing step. *Physical Review Fluids* **4**(10):103904.
3. Hu, W., Hickel, S., van Oudheusden, B. (2020). Influence of upstream disturbances on the primary and secondary instabilities in a supersonic separated flow over a backward-facing step. *Physics of Fluids* **32**(5): 56102.
4. Hu, W., Hickel, S., van Oudheusden, B. (2021). Low-frequency unsteadiness mechanisms in shock wave/turbulent boundary layer interactions over a backward-facing step. *Journal of Fluid Mechanics* **915**: A107.
5. Hu, W., Hickel, S., van Oudheusden, B. (2022). Unsteady mechanisms in shock wave boundary layer interactions over a forward-facing step. *Journal of Fluid Mechanics*.

6. Hu., W. (2020). Dynamics of a supersonic flow over a backward/forward-facing step. PhD Thesis, Delft University of Technology.
7. Hickel, S., Egerer, C. P. & Larsson, J. (2014). Subgrid-scale modeling for implicit large eddy simulation of compressible flows and shock-turbulence interaction. *Physics of Fluids* **26**(10): 106101.
8. Klein, M., Sadiki, A., Janicka, J. (2003). A digital filter based generation of inflow data for spatially developing direct numerical or large eddy simulations. *Journal of Computational Physics* **186**(2):652–665.
9. Priebe, S., Martin, M. P. (2012). Low-frequency unsteadiness in shock wave–turbulent boundary layer interaction. *Journal of Fluid Mechanics* **699**: 1– 49.
10. Pasquariello, V., Hickel, S., Adams, N. A. (2017). Unsteady effects of strong shock-wave/boundary- layer interaction at high Reynolds number. *Journal of Fluid Mechanics* **823**: 617–657.